01 Aug 2017

Unified Solution To Drained Expansion Of A Spherical Cavity In Clay And Sand

Lin Li

Jingpei Li

De'an Sun

Weibing Gong
Missouri University of Science and Technology, weibing.gong@mst.edu

Recommended Citation

L. Li et al., "Unified Solution To Drained Expansion Of A Spherical Cavity In Clay And Sand," *International Journal of Geomechanics*, vol. 17, no. 8, article no. 04017028, American Society of Civil Engineers, Aug 2017.
The definitive version is available at https://doi.org/10.1061/(ASCE)GM.1943-5622.0000909

Unified Solution to Drained Expansion of a Spherical Cavity in Clay and Sand

Lin Li[1]; Jingpei Li[2]; De'an Sun[3]; and Weibing Gong[4]

Abstract: This paper presents a novel unified solution to drained expansion of a spherical cavity in both clay and sand. The large-strain theory and a critical state model with a unified hardening parameter are used to describe the elastoplastic behavior of the soils after yielding. The elastoplastic constitutive tensor of the critical state model is developed to be a system of first-order differential equations for the drained expansion of a spherical cavity. The problem is formulated as an initial value problem in terms of the Lagrangian scheme by introducing an auxiliary variable and is solved numerically. With the present solution, curves for the expansion pressures, the distributions of stress components, and the stress paths are plotted to illustrate the different expansion responses in clay and sand. The proposed solution not only incorporates the dilatancy and peak strength of dense sand, but it can also reduce to the solution for clay and loose sand when ignoring the dilatancy and peak strength. Therefore, the present solution can be applied to interpret the cone penetration test and the pile installation, as well as to evaluate the pile end bearing capacity in various kinds of soils. **DOI: 10.1061/(ASCE)GM.1943-5622.0000909.**

Author keywords: Elastoplastic; Dilatancy; Auxiliary variable; Drained expansion; Expansion response.

Introduction

The cavity expansion theory has been widely used in geotechnical problems, such as the modeling of pile installation (Randolph et al. 1979; Vesic 1977; Roy et al. 1981; Randolph 2003) and the interpretation of the cone penetration test (Yu et al. 1996; Shuttle and Jefferies 1998; Chang et al. 2001; Cudmani and Osinov 2001; Salgado and Prezzi 2007). Because it is easy to implement, even with sophisticated soil models and larger strain theory (Shuttle 2007), the solution for cavity expansion is always a topic of interest for many researchers (Yu 2000; Cao et al. 2001; Shuttle 2007; Ghandeharioon et al. 2010; Frikha and Bouassida 2013; Zareifard and Fahimifar 2014). Great efforts have been devoted to improving the solutions of the cavity expansion problems since the pioneering works of Bishop et al. (1945) and Hill (1950). These improvements mainly focus on the development of new solution techniques (Carter et al. 1986; Collins et al. 1992; Salgado and Randolph 2001; Yu and Carter 2002; Chen and Abousleiman 2012, 2013; Zhou et al. 2014) and the application of more realistic constitutive models for geomaterials (Osinov and Cudmani 2001; Mantaras and Schnaid 2002; Zhao 2011; Yang and Zou 2011; Khalil 2013; Li et al. 2016a, b).

It is difficult to list all the research work dealing with the expansion of a cylindrical or spherical cavity. Hence, only some groundbreaking studies are briefly reviewed in this paper: Vesic (1977) derived a closed-from solution for cavity expansion in nonassociated Mohr-Coulomb soil considering the volume variation in the plastic region. Carter et al. (1986) and Yu and Houlsby (1991) presented analytical solutions for the expansion of spherical and cylindrical cavities from zero initial radii. The logarithmic strain and nonassociated Mohr-Coulomb criterion were adopted in their solutions to consider the large deformation and dilation characteristics of the soil in the plastic zone. Collins et al. (1992) proposed a similarity solution technique for cavity expansion from a zero initial radius in critical state soils. With this technique, the elastoplastic critical state constitutive models of soils can be incorporated in the cavity expansion solution to yield more realistic results. Yu (2000) performed a thorough and comprehensive review of the cavity expansion method using a variety of critical state models for both drained and undrained loading conditions. Zhao (2011) presented a unified theory for both cylindrical and spherical cavity expansions in cohesive-frictional micromorphic media. The elastoplastic behavior of the material was characterized by a phenomenological strain-gradient plasticity model with a generalized Mohr-Coulomb criterion. Chen and Abousleiman (2012, 2013) presented rigorous semianalytical solutions for drained and undrained cylindrical cavity expansions in Cam-clay soils without any approximation imposed on the constitutive relationship.

The previously mentioned studies have made significant contributions to the cavity expansion theory and have provided a better understanding of the cavity expansion responses in the surrounding soil. However, certain limitations still exist in those solutions, such as the elastic-perfectly plastic assumption and the simplified constitutive relation (Chen and Abousleiman 2012, 2013). As distinguished from the elastic-perfectly plastic materials, the elastoplastic behavior of soils is governed by the current stress state and the deformation history of the soil element (Cudmani and Osinov 2001). Nevertheless, the strengths of the soils in most available solutions were taken as constants and independent of the deformation history during cavity expansion because of the elastic-perfectly plastic assumption (Collins et al 1992; Yu 2000). Although some solutions used the critical state constitutive model to capture the elastoplastic response of the soils during cavity expansion (Chen and Abousleiman 2012, 2013), the peak strength and the negative/positive dilatancy of

[1]Ph.D. Student, Dept. of Geotechnical Engineering, Tongji Univ., Shanghai 200092, China. E-mail: lilin_sanmao@163.com

[2]Professor, Dept. of Geotechnical Engineering, Tongji Univ., Shanghai 200092, China (corresponding author). E-mail: lijp2773@163.com

[3]Professor, Dept. of Civil Engineering, Shanghai Univ., 149 Yanchang Rd., Shanghai 200072, China. E-mail: sundean06@163.com

[4]Master's Degree Candidate, Dept. of Geotechnical Engineering, Tongji Univ., Shanghai 200092, China. E-mail: weibingthomas@163.com

Note. This manuscript was submitted on May 16, 2016; approved on December 20, 2016; published online on March 1, 2017. Discussion period open until August 1, 2017; separate discussions must be submitted for individual papers. This paper is part of the ***International Journal of Geomechanics***, © ASCE, ISSN 1532-3641.

medium or dense sand during shear may not be properly described. Therefore, a reasonable drained solution for spherical cavity expansion in lightly or heavily dilatant sand is still not currently available, and little is known about the effects of dilatancy and peak strength on the cavity expansion responses.

The present work aims at developing a rigorous solution to the drained expansion of a spherical cavity in both clay and dilatant sand. For this, a unified hardening parameter-based critical state model (UHP model) (Yao et al. 2008) is used to describe the soil behavior during cavity expansion. The UHP model can properly reflect the dilatancy and peak strength of either lightly or heavily dilatant sand and can reduce to the modified Cam-clay (MCC) model for normally consolidated clay. Based on the rigorous constitutive relation of the UHP model, the problem is formulated by the Lagrangian scheme with the aid of an auxiliary variable suggested by Chen and Abousleiman (2013). The proposed solution can appropriately describe the expansion responses of a drained spherical cavity in both dilatant sand and nondilatant clay. It may provide a powerful tool capable of interpreting the cone penetration test and to assess the end bearing capacity of a pile in different kinds of soils.

Definition of the Problem

Problem Description

Consider a spherical cavity expanding in infinite isotropic drained soil with the in situ mean stress p_0. Initially, the radius of the cavity is a_0 and the internal pressure is p_0. The pressure inside the cavity is then increased to a value of σ_{ra} and the cavity expands to current radius a. A typical material particle moves outward from its original position r_0 to the current radial coordinate r in the spherical coordinate system, as shown in Fig. 1. During expansion, the soil adjacent to the cavity first experiences elastic deformation and then plastic yielding when the yield condition is satisfied. The corresponding cavity pressure at this stage is called the initial yielding pressure, denoted by σ_{rp}. After yielding, the cavity pressure increases progressively with the expansion of the cavity wall until the soil reaches the critical state. After the soil reaches the critical state, a further increase in the cavity wall will not cause an increase in cavity pressure. During the plastic expansion phase, a plastic zone is formed from the current cavity radius a to the elastoplastic (EP) boundary radius r_p. The symbol r_{p0} refers to the initial location of a soil particle that instantly

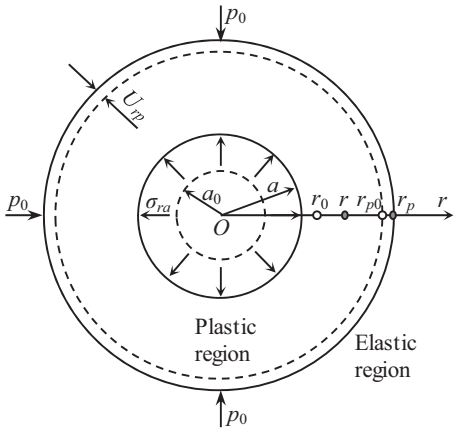

Fig. 1. Schematic for the drained expansion of a spherical cavity

becomes plastic. It is assumed that Hooke's elasticity law and small-strain theory govern the elastic behavior of the soil, whereas the elastoplastic behavior of the soil may be described by the large-strain theory and the UHP model for both sand and clay. This constitutive model is proposed by Yao et al. (2008) and will be shown later. Additionally, compressive stress and strain components are taken as positive quantities, and the term stress is interpreted as effective stress in this paper.

Soil Model

A general feature of sand behavior seen during shearing is that if a sample is initially in a very loose state, only strain hardening and volume contraction behavior will be observed, whereas a medium or dense sample may exhibit volume contraction, dilation, and peak strength behavior (Yao et al. 2004). To incorporate these features of sand and obtain a unified solution for cavity expansion in both clay and dilatant sand, a UHP critical model presented by Yao et al. (2008) is used to capture the elastoplastic feature of the soil during cavity expansion. The UHP model proposes a UHP H instead of the hardening parameter ε_v^p (plastic volumetric strain) in the Cam-clay model. The unified yield and plastic potential functions of the UHP model are the same as the Cam-clay mode, given as

$$f = \left(\frac{\eta}{M}\right)^2 - \frac{p_c}{p} + 1 = 0 \tag{1}$$

where p_c = mean effective yielding pressure; M = value of η at the characteristic state; and the stress parameter p and the stress ratio η are defined, respectively, as follows:

$$p = \frac{1}{3}\sigma_{ii} \tag{2a}$$

$$\eta = \sqrt{\frac{3}{2}\eta_{ij}\eta_{ij}} \tag{2b}$$

with

$$\eta_{ij} = \frac{\sigma_{ij} - p\delta_{ij}}{p} \tag{2c}$$

where σ_{ij} = stress tensor; and δ_{ij} = Kronecker's delta.

After introducing the UHP H, the yield function or the plastic potential function of the UHP model can be rewritten as

$$f = \frac{\lambda - \kappa}{1 + e_0}\ln\frac{p}{p_0} + \frac{\lambda - \kappa}{1 + e_0}\ln\left[1 + \left(\frac{\eta}{M}\right)^2\right] - H = 0 \tag{3}$$

where λ and κ = slopes of compression and swelling lines, respectively; e_0 = initial void ratio of soil for $p = p_0$; and the UHP H is defined as

$$H = \int dH = \int \frac{M^4}{M_f^4}\frac{M_f^4 - \eta^4}{M^4 - \eta^4} d\varepsilon_v^p \tag{4}$$

in which M_f = value of η at the failure state.

From Eq. (4), one can obtain

$$d\varepsilon_v^p = \frac{M_f^4}{M^4}\frac{M^4 - \eta^4}{M_f^4 - \eta^4} dH \tag{5}$$

Because H is a hardening parameter, dH is not less than zero. Hence, the following features can be deduced from Eq. (5): when $0 < \eta < M$, $d\varepsilon_v^p > 0$; when $\eta = M$, $d\varepsilon_v^p = 0$; and when $M < \eta < M_f$, $d\varepsilon_v^p < 0$. Especially when $\eta = 0$ or $M_f = M$, $dH = d\varepsilon_v^p$, the hardening parameter H becomes the plastic volumetric strain; thus, the UHP model simplifies to the Cam-clay model. Fig. 2 shows the comparisons of the measured results from the triaxial compression tests and the predicted results from the UHP model for dilatant sand and normally consolidated clay conducted by Yao et al. (2008). The good agreements in the figure demonstrate the validity and reliability of the UHP model. As indicated earlier, the behavior of both sand and clay during shearing are reasonably described by the hardening parameter H. The five soil parameters M_f, M, λ, κ, and v used in the UHP model can be determined by a loading and unloading isotropic compression test and a conventional triaxial compression test. One can refer to the literature (Yao et al. 2008) for more details about the UHP critical model.

Theoretical Considerations for the Problem

Solution in Elastic Region

For a spherical cavity problem, the equilibrium equation in the spherical coordinate system can be written as

$$\frac{\partial \sigma_r}{\partial r} + 2\frac{\sigma_r - \sigma_\theta}{r} = 0 \tag{6}$$

where σ_θ = tangential stress.

Based on Hooke's law, the elastic stress-strain relationship of the soil can be expressed in the increment form

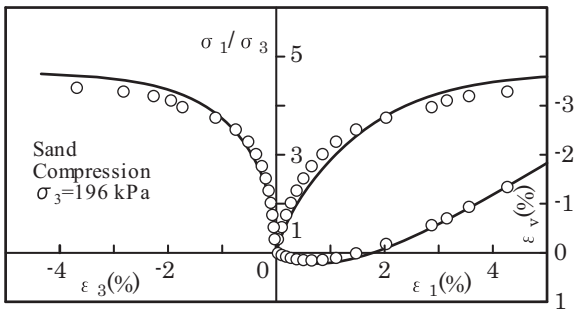

(a)

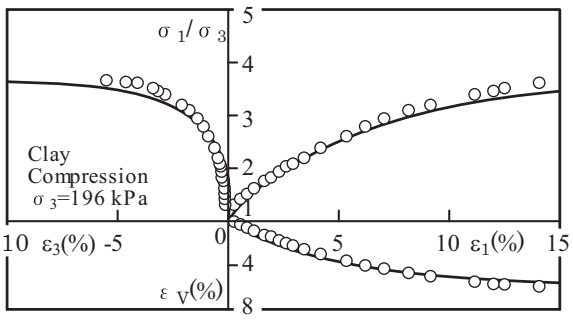

(b)

Fig. 2. Comparisons between measured results from triaxial compression tests and predicted results from the UHP model for sand and clay (data from Yao et al. 2008): (a) Toyoura sand; (b) Fujinomori clay

$$d\varepsilon_{ij}^e = \frac{1+v}{E} d\sigma_{ij} - \frac{v}{E} d\sigma_{\text{mm}} \delta_{ij} \tag{7}$$

where $E = 2G(1+v)$ = elastic modulus. In critical state models, the shear modulus G is defined as (Wood 1990)

$$G = \frac{3(1-2v)vp}{2(1+v)\kappa} \tag{8}$$

where v = specific volume; and ν = Poisson's ratio.

Combining Eqs. (6) and (7) with the small-strain theory, the radial displacement, U_r, and stress distributions in the elastic region can be obtained as (Yu 2000; Cao et al. 2001)

$$\sigma_r = p_0 + (\sigma_{\text{rp}} - p_0)\left(\frac{r_p}{r}\right)^3 \tag{9}$$

$$\sigma_\theta = p_0 - \frac{1}{2}(\sigma_{\text{rp}} - p_0)\left(\frac{r_p}{r}\right)^3 \tag{10}$$

$$U_r = \frac{\sigma_{\text{rp}} - p_0}{4G_0}\left(\frac{r_p}{r}\right)^3 r \tag{11}$$

where σ_{rp} = total radial stress at the EP boundary.

Stress and Displacement at the EP Boundary

From Eqs. (9) and (10), it can be seen that the mean stress p remains unchanged during the elastic phase, giving

$$p_p = p_0 \tag{12}$$

where p_p = mean effective stress at the EP boundary.

From Eq. (7), it can be deduced that the constant value of p means a zero volumetric strain increment in the elastic region, that is

$$v_p = v_0 \tag{13}$$

where v_p and v_0 = specific volume at the initial state and at the EP boundary, respectively.

Substituting Eq. (12) into Eq. (1), the stress ratio at the EP boundary, η_p, can be obtained as

$$\eta_p = M\sqrt{\text{OCR} - 1} \tag{14}$$

where OCR is the overconsolidation ratio, defined as p_{c0}/p_0. The pressure, p_{c0}, is the maximum mean preconsolidation stress.

From Eqs. (9), (10), and (14), the radial and tangential stresses at the EP boundary can be derived as

$$\sigma_{\text{rp}} = p_0\left(1 + \frac{2}{3}\eta_p\right) \tag{15}$$

$$\sigma_{\theta p} = p_0\left(1 - \frac{1}{3}\eta_p\right) \tag{16}$$

Substituting Eqs. (15) into Eq. (11), the radial displacement at the EP boundary, U_{rp}, can be obtained as

$$U_{\mathrm{rp}} = \frac{\sigma_{\mathrm{rp}} - p_0}{4G_0} r_p \tag{17}$$

EP Analysis

After initial yielding, the total strain increment of the soil, $d\varepsilon_{ij}$, consists of the elastic component, $d\varepsilon_{ij}^e$, and the plastic component, $d\varepsilon_{ij}^p$

$$d\varepsilon_{ij} = d\varepsilon_{ij}^e + d\varepsilon_{ij}^p \tag{18}$$

For the UHP model, the elastic strain increment can be calculated by Eq. (7), and the plastic strain increment can be obtained based on the associated plastic flow rule as follows:

$$d\varepsilon_{ij}^p = \Lambda \frac{\partial f}{\partial \sigma_{ij}} \tag{19}$$

where Λ is a scalar multiplier.

Applying the consistency condition to Eq. (3) gives

$$\Lambda = -\frac{M_f^4}{M^4}\frac{M^4 - \eta^4}{M_f^4 - \eta^4}\frac{(\partial f/\partial p)dp + (\partial f/\partial \eta)d\eta}{(\partial f/\partial H)(\partial f/\partial \sigma_{ii})} \tag{20}$$

where

$$\frac{\partial f}{\partial p} = \frac{\lambda - \kappa}{1 + e_0}\frac{1}{p} \tag{21a}$$

$$\frac{\partial f}{\partial \eta} = \frac{\lambda - \kappa}{1 + e_0}\frac{2\eta}{M^2 + \eta^2} \tag{21b}$$

$$\frac{\partial f}{\partial H} = -1 \tag{21c}$$

$$\frac{\partial p}{\partial \sigma_{ij}} = \frac{\delta_{ij}}{3} \tag{21d}$$

$$\frac{\partial \eta}{\partial \sigma_{ij}} = \frac{1}{2\eta}\frac{(3\eta_{ij} - \eta_{\mathrm{kl}}\eta_{\mathrm{kl}})\delta_{ij}}{p} \tag{21e}$$

with

$$\frac{\partial f}{\partial \sigma_{ij}} = \frac{\partial f}{\partial p}\frac{\partial p}{\partial \sigma_{ij}} + \frac{\partial f}{\partial \eta}\frac{\partial \eta}{\partial \sigma_{ij}} = \frac{\lambda - \kappa}{1 + e_0}\frac{1}{p}\left[\frac{\delta_{ij}}{3} + \frac{3\eta_{ij} - \eta_{\mathrm{kl}}\eta_{\mathrm{kl}}\delta_{ij}}{M^2 + \eta^2}\right] \tag{21f}$$

which results in

$$\frac{\partial f}{\partial \sigma_{ii}} = \frac{\lambda - \kappa}{1 + e_0}\frac{1}{p}\left(1 - \frac{3\eta_{\mathrm{kl}}\eta_{\mathrm{kl}}}{M^2 + \eta^2}\right) \tag{22}$$

Substituting Eqs. (21*a*)–(21*e*) and (22) into Eq. (20), the explicit expression of the scalar multiplier Λ can be obtained as

$$\Lambda = \frac{M_f^4}{M^4}\frac{M^4 - \eta^4}{M_f^4 - \eta^4}\left(\frac{\delta_{ij}}{3} + \frac{3\eta_{ij}}{M^2 - \eta^2}\right)d\sigma_{ij} \tag{23}$$

Consequently, the plastic strain increment can be given as

$$d\varepsilon_{ij}^p = \frac{c_p}{p^3}\frac{M_f^4(M^2 + \eta^2)^2}{M^4(M_f^4 - \eta^4)}\left[\frac{\delta_{ij}}{3} + \frac{3\eta_{ij} - \eta_{\mathrm{kl}}\eta_{\mathrm{kl}}\delta_{ij}}{M^2 + \eta^2}\right] \times \left[\frac{\delta_{ij}}{3} + \frac{3\eta_{ij} - \eta_{\mathrm{kl}}\eta_{\mathrm{kl}}\delta_{ij}}{M^2 + \eta^2}\right]d\sigma_{ij} \tag{24}$$

where $c_p = (\lambda - \kappa)/(1 + e_0)$.

Combining Eqs. (7), (18), and (24) and considering the geometric centrosymmetry of the spherical cavity expansion case, the elastoplastic constitutive relation for the problem can be expressed in the Lagrangian form as

$$\begin{Bmatrix} D\varepsilon_r \\ D\varepsilon_\theta \end{Bmatrix} = \begin{bmatrix} \frac{1}{E} + AA_r^2 & -\frac{2v}{E} + 2AA_rA_\theta \\ -\frac{v}{E} + AA_rA_\theta & \frac{1 - v}{E} + 2AA_\theta^2 \end{bmatrix} \begin{Bmatrix} D\sigma_r \\ D\sigma_\theta \end{Bmatrix} \tag{25}$$

where $D\varepsilon_r$, $D\varepsilon_\theta$ and $D\sigma_r$, $D\sigma_\theta$ = strain and stress increments of a given material particle in the radial and tangential directions, respectively. The expressions of A_r, A_θ, and A are as follows:

$$A_r = \frac{1}{3} + \frac{3\eta_r - \eta_{\mathrm{kl}}\eta_{\mathrm{kl}}}{M^2 + \eta^2} \tag{26a}$$

$$A_\theta = \frac{1}{3} + \frac{3\eta_\theta - \eta_{\mathrm{kl}}\eta_{\mathrm{kl}}}{M^2 + \eta^2} \tag{26b}$$

$$A = \frac{c_p}{p}\frac{M_f^4}{M^4}\frac{(M^2 + \eta^2)^2}{M_f^4 - \eta^4} \tag{26c}$$

The performing matrix inversion calculation to Eq. (25), noting that the volumetric increments for the spherical cavity expansion problem is $D\varepsilon_v = -Dv/v = D\varepsilon_r + 2D\varepsilon_\theta$, and the EP constitutive relation for the case can be simplified as

$$D\sigma_r = \frac{1}{B}\left[B_{11}\left(-\frac{Dv}{v}\right) + (B_{12} - 2B_{11})D\varepsilon_\theta\right] \tag{27a}$$

$$D\sigma_\theta = \frac{1}{B}\left[B_{21}\left(-\frac{Dv}{v}\right) + (B_{22} - 2B_{21})D\varepsilon_\theta\right] \tag{27b}$$

where

$$B_{11} = E(2EAA_\theta^2 + 1 - v) \tag{28a}$$

$$B_{12} = 2E(v - EAA_rA_\theta) \tag{28b}$$

$$B_{21} = E(v - EAA_rA_\theta) \tag{28c}$$

$$B_{22} = E(EAA_r^2 + 1) \tag{28d}$$

$$B = EAA_r^2(1 - v) + 4EvAA_rA_\theta + 2EAA_\theta^2 + 1 - v - 2v^2 \tag{28e}$$

To incorporate the effect of a large deformation in the plastic zone, the logarithmic strains are adopted, defined as

$$\varepsilon_r = -\ln\frac{dr}{dr_0} \tag{29a}$$

$$\varepsilon_\theta = -\ln\frac{r}{r_0} \tag{29b}$$

With the EP boundary conditions given by Eqs. (15)–(17), the three unknown variables (σ_r, σ_r, and v) for the problem can be determined by combining Eqs. (1), (27a), (27b), (29a), and (29b). However, Eqs. (1), (27a), (27b), (29a), and (29b) are defined in terms of the Eulerian description. Hence, to formulate the problem, it is necessary to transform Eqs. (1), (27a), (27b), (29a), and (29b) into the Lagrangian scheme. Following Chen and Abousleiman (2013), this can be achieved in the following by introducing an auxiliary variable, ξ, defined as:

$$\xi = \frac{U_r}{r} = \frac{r - r_0}{r} \tag{30}$$

Introducing Eq. (30) into Eqs. (1) and (29a), and (29b) gives

$$\frac{D\sigma_r}{D\xi}\left(-\frac{U_r}{r^2} + \frac{1}{r}\frac{dU_r}{dr}\right) + 2\frac{\sigma_r - \sigma_\theta}{r} = 0 \tag{31}$$

$$\varepsilon_r = \varepsilon_v - 2\varepsilon_\theta = -\ln\left(\frac{v}{v_0}\right) + 2\ln\left(\frac{r}{r_0}\right) = \ln\left[\frac{v_0}{v(1-\xi)^2}\right] \tag{32a}$$

$$\varepsilon_\theta = \ln(1-\xi) \tag{32b}$$

Substituting Eq. (32b) into Eq. (27a), and combining with Eq. (31), yields

$$-2(\sigma_r - \sigma_\theta) = \left[-\frac{B_{11}}{B}\frac{Dv}{vD\xi} - \frac{B_{12} - 2B_{11}}{B(1-\xi)}\right]\left(-\xi + \frac{dU_r}{dr}\right) \tag{33}$$

On the other hand, Eqs. (29a) and (32a) can be combined and rearranged to give

$$\frac{dU_r}{dr} = 1 - \frac{v_0}{v(1-\xi)^2} \tag{34}$$

Combining Eqs. (33) and (34), one can obtain

$$\frac{Dv}{D\xi} = \frac{Bv}{B_{11}}\left\{\frac{2(\sigma_r - \sigma_\theta)}{1 - \xi - v_0/\left[v(1-\xi)^2\right]} + \frac{2B_{11} - B_{12}}{B(1-\xi)}\right\} \tag{35a}$$

Substituting Eqs. (32b) and (35a) into Eq. (27a) and (27b), the constitutive relation can be expressed with the auxiliary variable as

$$\frac{D\sigma_r}{D\xi} = -\frac{2(\sigma_r - \sigma_\theta)}{1 - \xi - v_0/\left[v(1-\xi)^2\right]} \tag{35b}$$

$$\frac{D\sigma_\theta}{D\xi} = -\frac{B_{21}}{B_{11}}\left\{\frac{2(\sigma_r - \sigma_\theta)}{1 - \xi - v_0/\left[v(1-\xi)^2\right]} + \frac{2B_{11} - B_{12}}{B(1-\xi)}\right\} - \frac{B_{22} - 2B_{21}}{B(1-\xi)} \tag{35c}$$

In addition, the EP boundary conditions should be described as the initial conditions in terms of the Lagrangian scheme. With the definition of the auxiliary variable, the initial conditions can be obtained from Eqs. (15)–(17), given as

$$\sigma_{\xi_p} = p_0\left(1 + \frac{2}{3}\eta_p\right) \tag{36a}$$

$$\sigma_{\xi_p} = p_0\left(1 - \frac{1}{3}\eta_p\right) \tag{36b}$$

$$v_{\xi_p} = v_0 \tag{36c}$$

with

$$\xi_p = \frac{\sigma_{\xi_p} - p_0}{4G_0} \tag{36d}$$

Consequently, the problem is finally formulated as a set of first-order ordinary differential equations given by Eqs. (35a)–(35c) with the initial conditions given by Eqs. (36a)–(36d). Because the three unknown variables σ_r, σ_θ, and v, only depend on the single auxiliary variable ξ, the governing equations can be solved numerically as an initial value problem with these variables starting at ξ_p. Additionally, it should be noted that results are expressed with respect to the auxiliary variable ξ. To express the results in terms of the particle position r, the auxiliary variable ξ can be associated with the particle position r by recalling Eqs. (30) and (34), which can be combined and rearranged to give

$$\frac{dr}{r} = \frac{d\xi}{1 - \xi - v_0/\left[v(\xi)(1-\xi)^2\right]} \tag{37}$$

Integrating Eq. (37) from the cavity wall to any location in the plastic region, the relationship between the ξ and r can be obtained as

$$\frac{r}{a} = \exp\left\{\int_{\xi(a)}^{\xi} \frac{d\xi}{1 - \xi - v_0/\left[v(\xi)(1-\xi)^2\right]}\right\} \tag{38}$$

Results and Discussion

With the aim of illustrating the different expansion responses in clay and sand, a parametric study was performed using the proposed solution. Three groups of parameters considered to be representative of loose, medium, and dense sands were selected in the study. As mentioned previously, if $M = M_f$, then these parameters also were considered to be representative of lightly, moderately, and heavily overconsolidated clays. The detailed information about the parameters used for analyses is summarized in Table 1. It should be emphasized that the intention here is not to study the general expansion response of a spherical cavity, but to explore the different expansion responses in clay and sand. Hence, the general expansion response of a drained spherical cavity will not be described and explained repeatedly in this study. In addition, because the UHP model reduces to the MCC model for loose sand ($M = M_f$), the expansion response curve for loose sand completely overlaps the curve for lightly overconsolidated clay with the same soil parameters in the following figures.

Table 1. Information of Soil Parameters Used for the Parametric Study

	$\lambda = 0.13$, $\kappa = 0.02$, $v = 0.3$					
Soil type	M_f	M	OCR	p_0 (kPa)	G_0 (kPa)	υ_0
Loose sand	1.2	1.2	1.2	120	5,374	1.94
Medium sand	1.66	1.2	3	120	5,094	1.83
Dense sand	1.79	1.2	7	120	4,836	1.75

Note: OCR = overconsolidated ratio.

Typical pressure-expansion relationships are presented for different types of sand and clay in Fig. 3, in which the expansion pressure σ_{ra} and the current cavity radius a are normalized with respect to p_0 and a_0, respectively. As seen in this figure, all the pressure-expansion curves are similar to each other, which demonstrate that the expansion responses are similar in both sand and clay. Nonetheless, except in loose sand and the lightly overconsolidated clay ($M = M_f$), the expansion pressure in sand is generally higher than it is in clay with the same soil parameter other than $M \neq M_f$. The higher expansion pressure in sand can be attributed to the peak strength and dilatancy of the medium and dense sand, which are not exhibited in clay during shearing.

Fig. 4 shows the variation of the normalized EP boundary radius, r_p/a, with the normalized instant cavity radius, a/a_0, for both sand and clay. This figure shows that although the dilatant sand and overconsolidated clay are in the same initial consolidation condition, a larger plastic zone is developed in the dilatant sand (medium and dense sand) compared with the plastic zone developed in the overconsolidated clay (moderately and heavily overconsolidated clay). This means that the medium or dense sand around the cavity is *pushed* outward more obviously because of the dilatancy during cavity expansion.

Additionally, Figs. 3 and 4 show that in sand and clay an increase in OCR results in an increase in the expansion pressure, leading to a decrease in the plastic zone, which is consistent with the results reported by Chen and Abousleiman (2013) for drained expansion of a cylindrical cavity in the MCC soil. This phenomenon clearly indicates that the OCR plays a fundamental role in soil behavior, greatly affecting the expansion responses during cavity expansion.

The stress paths (SPs) in the $p - q$ plane for a soil element located at the cavity wall during cavity expansion for sand and clay with different OCRs are plotted in Figs. 5–7. All the stresses in the figures have been normalized by p_0. The Points O, Y, and F denote the in situ stress point, the yield stress point, and the failure stress point, respectively. As seen in these figures, all the SPs first move vertically and the soils remain elastic until the SPs hit the initial yield locus at Point P. After yielding, the SPs of the loose sand, the lightly overconsolidated clay, and the medium sand move upward to the right until the SPs reach the critical state line (CSL) at Point F, which implies that the soils exhibit the strain-hardening behavior during the entire expansion phase. However, the SPs of the moderately and heavily overconsolidated clays as well as the dense sand move to the right and pass through the CSL inside the initial yield curve, Then, the SPs move outside the initial yield curve (IYC) and gradually approach the CSL at Point F, which demonstrates that these soils experience plastic softening then hardening during the cavity expansion.

It is also interesting to note in Figs. 6 and 7 that before yielding, the SP of the dilatant sand overlaps the SP of the overconsolidated clay, because the stress components are the same for both clay and sand during the elastic phase. However, after yielding, because the medium or dense sand exhibits the peak strength behavior, the SP of the dilatant sand is always located above the SP of the overconsolidated clay with the same stress history, and the CSL of the dilatant

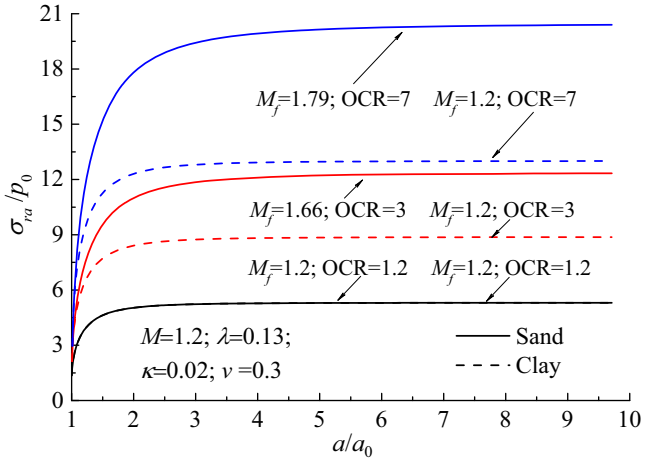

Fig. 3. Variation of normalized expansion pressure with cavity radius for different types of sands and clays

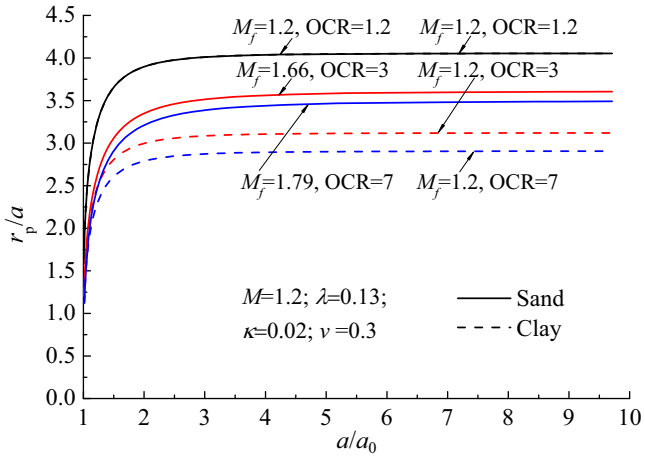

Fig. 4. Variation of normalized plastic zone radius with cavity radius for different types of sands and clays

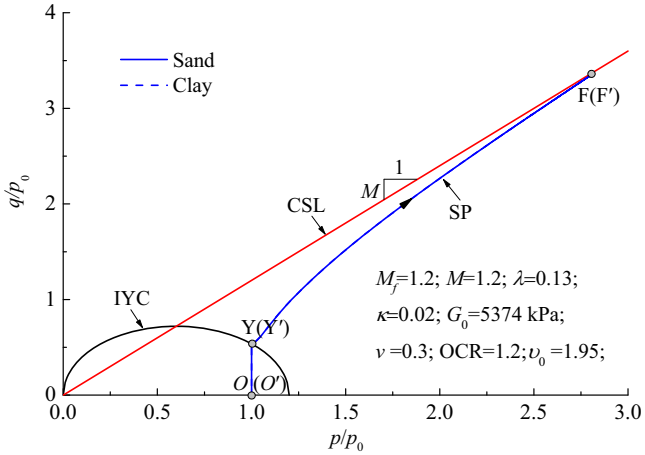

Fig. 5. SP of a soil element located at the cavity wall in the $p - q$ plane for the loose sand and the slightly overconsolidated clay (Note: CSL = critical state line; IYC = initial yield curve)

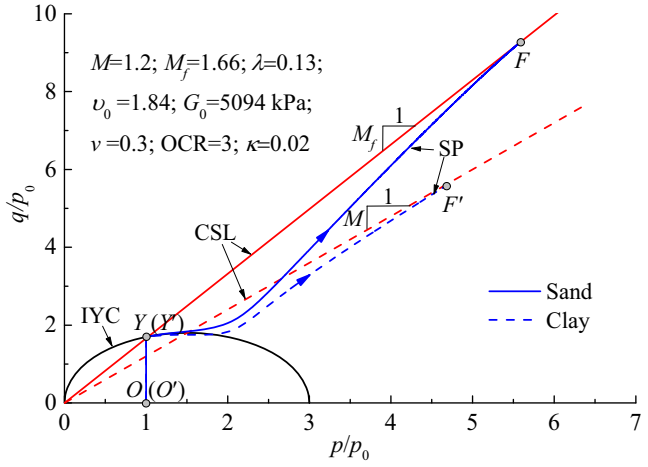

Fig. 6. SP of a soil element located at the cavity wall in the $p-q$ plane for the medium sand and the moderately overconsolidated clay (Note: CSL = critical state line; IYC = initial yield curve)

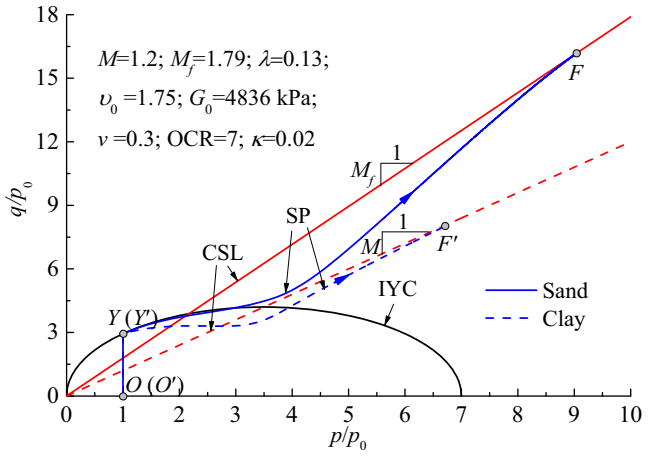

Fig. 7. SP of a soil element located at the cavity wall in the $p-q$ plane for the dense sand and the heavily overconsolidated clay (Note: CSL = critical state line; IYC = initial yield curve)

sand lies above the CSL of overconsolidated clay. This explains why a larger expand pressure is developed in the dilatant sand compared with the expand pressure developed in the overconsolidated clay with the same soil parameters other than $M \neq M_f$.

The distributions of normalized radial and tangential stresses as well as the specific volume around the cavity at the instant of $a/a_0 = 2$ for different types of sand and clay are comprehensively shown in Figs. 8–10. The stress components have been normalized with respect to p_0 and the radial axis to the current cavity radius a. Because the cavity expands in a self-similar manner (Collins et al. 1992), the curves in Figs. 8–10 also represent the stress and volume changes experienced by a material particle located at the cavity wall. As seen in Figs. 8–10, the stress components in both sand and clay decrease rapidly with r/a_0 in the plastic zone and gradually approach the in situ mean stress in the elastic region. It can also be found that the specific volumes of the loose sand and clays increase slightly with r/a_0 in the plastic zone, whereas the specific volumes of the medium and dense sand decrease significantly and then slightly with r/a_0 in the plastic zone. This demonstrates that the dilatant sand experiences both volume contraction and dilation during

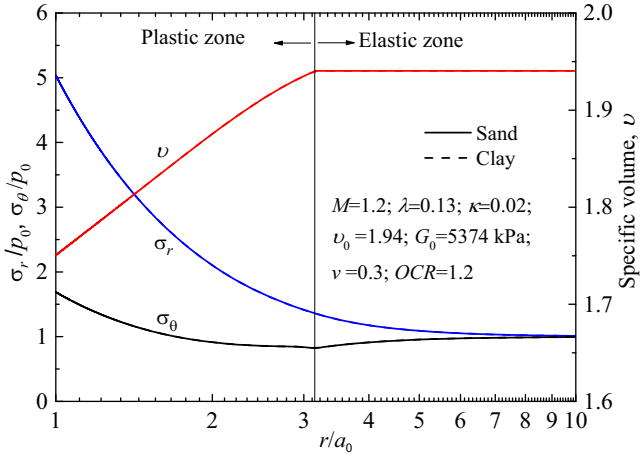

Fig. 8. Distributions of the specific volume and normalized stress components and around the cavity in the loose sand and slightly overconsolidated clay at the instant cavity radius of $a/a_0 = 2$

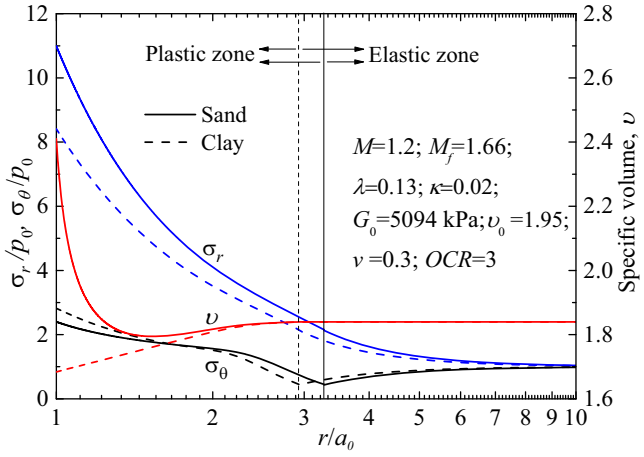

Fig. 9. Distributions of the specific volume and normalized stress components and around the cavity in the medium sand and moderately overconsolidated clay at the instant cavity radius of $a/a_0 = 2$

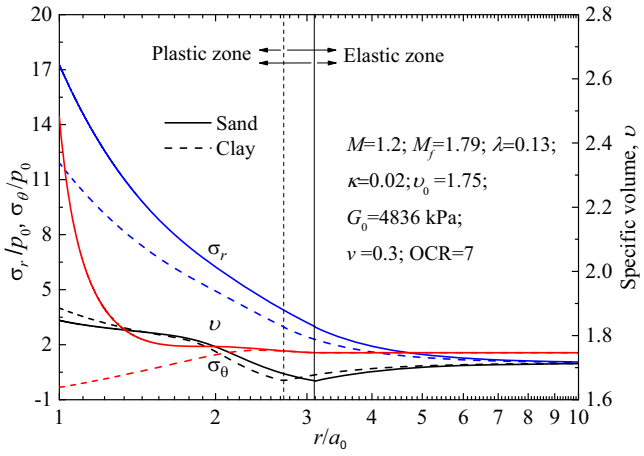

Fig. 10. Distributions of the specific volume and normalized stress components and around the cavity in the dense sand and heavily overconsolidated clay at the instant cavity radius of $a/a_0 = 2$

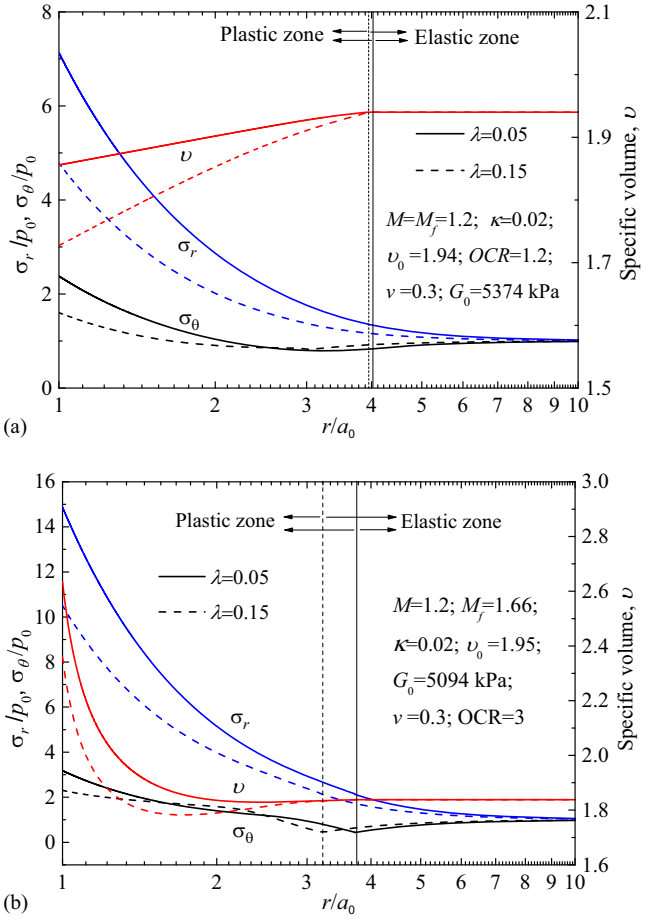

Fig. 11. Effect of parameter λ on distributions of the specific volume and normalized stress components around the cavity at the instant cavity radius of $a/a_0 = 2$: (a) normally consolidated clay or loose sand; (b) dilatant sand

cavity expansion, whereas the loose sand and clays only exhibit volume contraction behavior. Moreover, Figs. 9 and 10 also show that a larger plastic zone is developed in the dilatant sand compared with the plastic zone developed in the clay, which further indicates that the dilatancy of dilatant sand amplifies the squeezing effect around the cavity. It is also demonstrated that the dilatancy of the dilatant sand can be effectively reflected by the proposed solution.

The parameter λ of sand is generally much smaller than that of clay due to the different compression behaviors of sand and clay. To investigate the effects of the parameter λ on the cavity expansion responses, Fig. 11 shows the distributions of the specific volume and the normalized stress components around the cavity for clay and sand with different values of λ, respectively. As seen in the figure, the smaller value of λ results in larger stress components and smaller volume contraction around the cavity, i.e., a stronger expansion response. This is because the slope of the compression line λ represents the soil compressibility, and the soil with a smaller value of λ displays a stiffer and stronger response during cavity expansion. Moreover, it can be seen that the EP boundary radius is larger for the soil with a smaller value of λ because of its lower compressibility.

Conclusions

In this paper, a unified solution was developed based on a unified critical state model to capture the drained expansion responses for spherical cavities in both sand and clay. This solution can properly reflect the peak strength and dilatancy of medium and dense sands during cavity expansion and reduce to the MCC model-based solution for normally consolidated clay and loose sand. With the proposed solution, a parametric study was performed to illustrate the different expansion responses in sand and clay. The main conclusions are listed as follows:

1. Because of the peak strength of medium and dense sand, a higher expansion pressure is developed in the dilatant sand compared with the expansion pressure in the clay under the same initial consolidation condition.
2. The dilatancy of the dilatant sand amplifies the squeezing effect around the cavity; thus, the plastic region in the dilatant sand is generally larger than that in the clay with the same soil parameter other than $M \neq M_f$.
3. The stress history of soil has a pronounced effect on the responses of drained expansion of a spherical cavity. A higher value of OCR results in a larger expansion pressure and a smaller plastic region around the cavity.
4. The proposed unified solution not only captures the expansion responses for both sand and clay, but it also can incorporate the effects of the soil stress history. Hence, the present solution is applicable to cavity expansion problems, such as the cone penetration test, the pile installation, and the pile loading test, in many types of soils with different dilatancy.

Acknowledgments

The authors are grateful for the financial support provided by the National Natural Science Foundation of China (Grant 41272288) for this research work. The anonymous reviewers' comments have improved the quality of this paper and are also gratefully acknowledged.

References

Bishop, R. F., Hill, R., and Mott, N. F. (1945). "The theory of indentation and hardness tests." *Proc. Phys. Soc.*, 57(3), 147–159.

Cao, L. F., Teh, C. I., and Chang, M. F. (2001). "Undrained cavity expansion in modified Cam clay I: Theoretical analysis." *Géotechnique*, 51(4), 323–334.

Carter, J. P., Booker, J. R., and Yeung, S. K. (1986). "Cavity expansion in cohesive frictional soils." *Géotechnique*, 36(3), 349–353.

Chang, M. F., Teh, C. I., and Cao, L. F. (2001). "Undrained cavity expansion in modified Cam clay II: Application to the interpretation of the piezocone test." *Géotechnique*, 51(4), 335–350.

Chen, S. L., and Abousleiman, Y. N. (2012). "Exact undrained elastoplastic solution for cylindrical cavity expansion in modified Cam Clay soil." *Géotechnique*, 62(5), 447–456.

Chen, S. L., and Abousleiman, Y. N. (2013). "Exact drained solution for cylindrical cavity expansion in modified Cam Clay soil." *Géotechnique*, 63(6), 510–517.

Collins, I. F., Pender, M. J., and Wang, Y. (1992). "Cavity expansion in sands under drained loading conditions." *Int. J. Numer. Anal. Methods Geomech.*, 16(1), 3–23.

Cudmani, R., and Osinov, V. A. (2001). "The cavity expansion problem for the interpretation of cone penetration and pressuremeter tests." *Can. Geotech. J.*, 38(3), 622–638.

Frikha, W., and Bouassida, M. (2013). "Cylindrical cavity expansion in elastoplastic medium with a variable potential flow." *Int. J. Geomech.*, 10.1061/(ASCE)GM.1943-5622.0000166, 9–15.

Ghandeharioon, A., Indraratna, B., and Rujikiatkamjorn, C. (2010). "Analysis of soil disturbance associated with mandrel-driven prefabricated vertical drains using an elliptical cavity expansion theory." *Int. J. Geomech.*, 10.1061/(ASCE)GM.1943-5622.0000027, 53–64.

Hill, R. (1950). *The mathematical theory of plasticity*, Oxford University Press, London.
Khalil, I. (2013). "New pressuremeter test analysis based on critical state mechanics." *Int. J. Geomech.*, 10.1061/(ASCE)GM.1943-5622.0000257, 625–635.
Li, J., Li, L., Sun, D., and Rao, P. (2016a). "Analysis of undrained cylindrical cavity expansion considering three-dimensional strength of soils." *Int. J. Geomech.*, 10.1061/(ASCE)GM.1943-5622.0000650, 04016017.
Li, L., Li, J. P., and Sun, D. A. (2016b). "Anisotropically elasto-plastic solution to undrained cylindrical cavity expansion in K_0-consolidated clay." *Comput. Geotech.*, 73, 83–90.
Mantaras, F. M., and Schnaid, F. (2002). "Cylindrical cavity expansion in dilatant cohesive-frictional materials." *Géotechnique*, 52(5), 337–348.
Osinov, V. A., and Cudmani, R. (2001). "Theoretical investigation of the cavity expansion problem based on a hypoplasticity model." *Int. J. Numer. Anal. Methods Geomech.*, 25(5), 473–495.
Randolph, M. F. (2003). "Science and empiricism in pile foundation design." *Géotechnique*, 53(10), 847–875.
Randolph, M. F., Carter, J. P., and Wroth, C. P. (1979). "Driven piles in clay-the effects of installation and subsequent consolidation." *Géotechnique*, 29(4), 361–393.
Roy, M., Blanchet, R., and Tavenas, F. (1981). "Behaviour of a sensitive clay during pile driving." *Can. Geotech. J.*, 18(1), 67–85.
Salgado, R., and Prezzi, M. (2007). "Computation of cavity expansion pressure and penetration resistance in sands." *Int. J. Geomech.*, 10.1061/(ASCE)1532-3641(2007)7:4(251), 251–265.
Salgado, R., and Randolph, M. F. (2001). "Analysis of cavity expansion in sand." *Int. J. Geomech.*, 10.1061/(ASCE)1532-3641(2001)1:2(175), 175–192.
Shuttle, D. (2007). "Cylindrical cavity expansion and contraction in Tresca soil." *Géotechnique*, 57(3), 305–308.
Shuttle, D., and Jefferies, M. (1998). "Dimensionless and unbiased CPT interpretation in sand." *Int. J. Numer. Anal. Methods Geomech.*, 22(5), 351–391.
Vesic, A. S. (1977). *Design of pile foundations*, National Research Council, Washington, DC.
Wood, D. M. (1990). *Soil behaviour and critical state soil mechanics*, Cambridge University Press, Cambridge, U.K.
Yang, X. L., and Zou, J. F. (2011). "Cavity expansion analysis with nonlinear failure criterion." *Proc. Inst. Civ. Eng.Geotech. Eng.*, 164(1), 41–49.
Yao, Y. P., Sun, D. A., and Luo, T. (2004). "A critical state model for sands dependent on stress and density." *Int. J. Numer. Anal. Methods Geomech.*, 28(4), 323–337.
Yao, Y. P., Sun, D. A., and Matsuoka, H. (2008). "A unified constitutive model for both clay and sand with hardening parameter independent on stress path." *Comput. Geotech.*, 35(2), 210–222.
Yu, H., and Carter, J. (2002). "Rigorous similarity solutions for cavity expansion in cohesive-frictional soils." *Int. J. Geomech.*, 10.1061/(ASCE)1532-3641(2002)2:2(233), 233–258.
Yu, H., Schnaid, F., and Collins, I. (1996). "Analysis of cone pressuremeter tests in sand." *J. Geotech. Eng.*, 10.1061/(ASCE)0733-9410(1996)122:8(623), 623–632.
Yu, H. S. (2000). *Cavity expansion methods in geomechanics*, Kluwer Academic, Dordrecht, Netherlands.
Yu, H. S., and Houlsby, G. T. (1991). "Finite cavity expansion in dilatant soils: Loading analysis." *Géotechnique*, 41(2), 173–183.
Zareifard, M., and Fahimifar, A. (2014). "Elastic–brittle–plastic analysis of circular deep underwater cavities in a Mohr-Coulomb rock Mass considering seepage forces." *Int. J. Geomech.*, 10.1061/(ASCE)GM.1943-5622.0000400, 04014077.
Zhao, J. D. (2011). "A unified theory for cavity expansion in cohesive-frictional micromorphic media." *Int. J. Solids Struct.*, 48(9), 1370–1381.
Zhou, H., Liu, H. L., and Kong, G. Q. (2014). "Analytical solution of undrained cylindrical cavity expansion in saturated soil under anisotropic initial stress." *Comput. Geotech.*, 55, 232–239.